RSC Advances

ROYAL SOCIETY OF CHEMISTRY

www.rsc.org/advances

Table of contents entry：
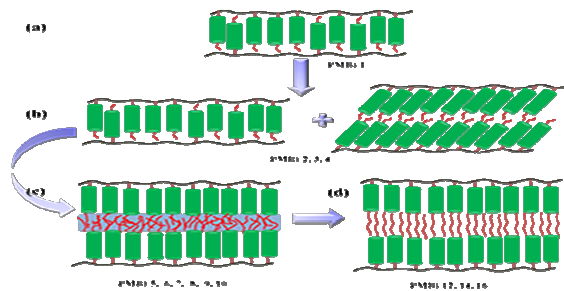
Highlight

➢ the alkoxy tail plays an important role in the phase behavior of the SCLCPs based on biphenyl mesgoen without the spacer

RSC Advances

RSC Publishing

Influence of Alkoxy Tail Length on the Phase Behaviors of Side-Chain Liquid Crystalline Polymers without the Spacer

Bin Ni, Junqiu Liao, Sheng Chen*, Hai-liang Zhang*

A series of end-on side-chain liquid crystalline polymers (SCLCPs) based on the biphenyl mesogen which were directly attached to the polymer backbone without the flexible spacer, poly(4,4'-alkoxybiphenylyl methacrylate) (PMBi-m, m = 1, 2, 3, 4, 5, 6, 7, 8, 9, 10, 12, 14, 16) were successfully synthesized by free radical polymerization. The chemical structures of the monomers were confirmed by ^{1}H NMR and Mass Spectrometry. The molecular characterizations of the polymers were performed with ^{1}H NMR, GPC and TGA. The phase behaviors were investigated by the combination of techniques including DSC, POM and 1D/2D WAXD. The experimental results showed that the alkoxy tail played an important role in the phase behaviors of the SCLCPs without the spacer. Firstly, all polymers form the smectic phase. Secondly, the clearing temperatures decrease with a small odd-even effect as the length of the alkyl tail increases and then increase slightly. Last, compared with the influence of the alkyl spacer length on liquid crystal properties of end-on SCLCPs with the biphenyl mesogen, the end-on SCLCPs without the spacer and with the different alkyl tail length (PMBi-m) exhibit the high glass transition temperature and the stable LC phase.

1. Introduction

Side-chain liquid crystalline polymers (SCLCPs) have been extensively studied not only because of their potentiality as materials in many fields, such as optical data storage, optic, electro-optic, nonlinear optic devices, photomechanical etc, but also because they provide a testing challenge to our understanding of the structural factors that promote liquid crystallinity in polymeric system.[1-14]

It is well known that the properties of SCLCPs depend on the nature of the polymer backbone, the nature of the mesogenic groups and on the length of the flexible spacers.[15-17] For the flexible spacer, Ringsdorf and Finkelmann pointed out that the flexible spacer inserted between main chain and mesogenic side groups was indispensable in order for a SCLCP to achieve LC phase since it decoupled the interaction of side chain and polymer backbone, which disrupted the ordered packing of the side mesogens.[18-19] This "decoupling concept" can explain why a few end-on SCLCPs without the spacer cannot form the LC phase (see **Fig.1**)[20-22] and has become a useful guideline for the molecular design of SCLCPs.

Key Laboratory of Polymeric Materials and Application Technology of Hunan Province, Key Laboratory of Advanced Functional Polymer Materials of Colleges, Universities of Hunan Province, College of Chemistry, Xiangtan University, Xiangtan 411105, Hunan Province, China. Email: huaxuechensheng@163.com, zhl1965@xtu.edu.cn

However, on the basis of relative literatures, there are many end-on SCLCPs without the spacer to exhibit the LC phase (see **Fig.2**).[20, 23-29] Meantime, as can be seen from **Fig.1** and **Fig.2**, although some SCLCPs without the spacer cannot show the LC phase, when the alkoxy tails attached to the mesgeon, the polymer would present the LC phase, such as, P1 and P17, P2 and P15. Thus, the alkyl tail plays a very important role in the formation of LC phase structure for the SCLCPs without spacer, even identical with the flexible spacer. For example, recently, Chen et al. have report the synthesis and characterization of a new end-on side-chain liquid crystalline polymer (SCLCP), poly[4-(4'-alkoxyphenyloxymethylene)styrene], with the flexible rod-like mesogenic side-chain directly attached to the polymer backbone without flexible spacer (see **Fig.2** P21).[27] The results indicated that when the length of alkyl tail (m) was 2, 4, 6, the polymers were amorphous. When m=8, 12 and 16, the polymers could self-assembly into the smectic A phase. All of these indicated that the alkyl tail thought to be a factor influencing the microstructure, and thus the mesomorphic behavior of end-on SCLCPs without the spacer.

In order to design new materials having targeted properties for applications, we should first develop and understand knowledge-based rules relating polymer structure to LC properties. Although there is much data in the literature describing the LC properties of LC materials, there are few studies in which the length alkyl tail is varied in a systematic fashion for a given backbone and mesogenic group.[30-31] In the present work, we intend to describe a detail study of the LC behavior of a series of polymethacrylates containing

biphenyl side chains without the spacer (PMBi-m, in which m denotes the number of methylene groups in the flexible tail, m=1, 2, 3, 4, 5, 6, 7, 8, 9, 10, 12, 14, 16, see **Scheme 1**). Biphenyl has been used in this study because it is the most widely used mesogenic core and has been attached to a wide range of backbone types. Such a study of the phase behavior of the complete homologous series would allow for the rational design of new polymers having tailored phase behavior.
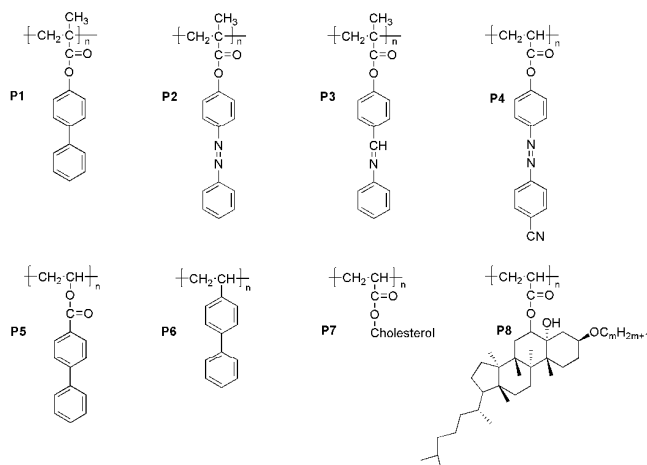
Fig.1 Chemical structures of amorphous polymers.
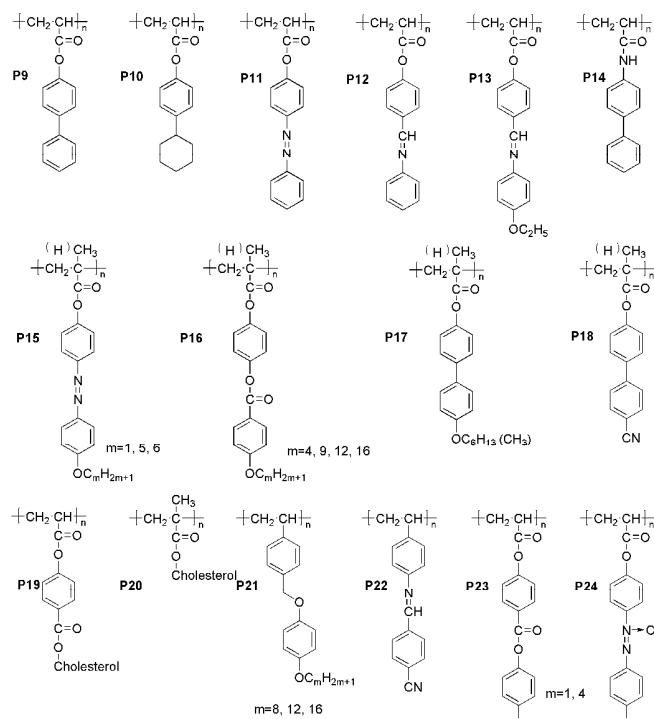
Fig.2 Chemical structures of end-on side-chain liquid crystalline polymers.

2. Experimental

2.1. Materials

Anhydrous tetrahydrofuran (THF) was distilled from sodium benzophenone ketyl under argon and used immediately. 2, 2 azobisisobutyronitrile (AIBN) was freshly recrystallised from methanol. 4, 4'-Diphenol (98%, Alfa Aesar) and bromoalkanes together with other reagents and solvents were used as received without further purification.

2.2. Synthesis of Monomers

For convenience, the 4, 4'-alkoxybiphenylyl methacrylate monomers were named MBi-m (m=1, 2, 3, 4, 5, 6, 7, 8, 9, 10, 12, 14, 16), and the corresponding polymers were named PMBi-m. The synthetic route of monomers MBi-m is shown in **Scheme 1**. The experimental details are described as follows:

4-Alkyloxy-4'-hydroxybiphenyls: 4-Alkyloxy-4-hydroxybiphenyls were synthesized by standard methods from 4, 4'-biphenyldiol with bromoalkanes in the presence of K_2CO_3. The mixture was heated for 12 h in 55 °C, next the reaction mixture poured into a large amount of water to precipitate products. The products were purified by precipitation in water from THF solution three times. At last, the crude products were purified by column chromatograph (silica gel, CH_2Cl_2). The final product of 4-alkoxybiphenol was white powder.

4, 4'-Alkoxybiphenylyl methacrylate: 1mol Methacryloyl chloride and 5 mol TEA were dissolved in 200mL THF. Under intense stirring at 0 °C, 1 mol 4-alkyloxy-4-hydroxybiphenyls was slowly added into the above solution over a period of 2 h. The mixture was further stirred at room temperature for 12 h, the mixture was filtered in order to remove inorganic salts. Then the reaction mixture was precipitated into a large amount of water, and was filtered. At last, the crude products were purified by column chromatograph (silica gel, CH_2Cl_2). The characterization data of MBi-10 was as follows: ^{1}H NMR ($CDCl_3$): δ=0.88–1.89 (m, 19H, alkoxy H), 2.1–2.3(s, 3H, C=C-CH_3), 3.9-4.1(t, 2H, -O-CH_2-), 5.5–6.5(2d, 2H, CH_2=C-), 6.8-7.8(m, 8H, Ar-H). Mass Spectrometry (MS) (m/z) [M] Calcd for $C_{26}H_{34}O_3$, 394.24.; found, 394.353.

2.3. Synthesis of Polymers

All polymers was obtained by conventional solution radical polymerization (see **Scheme 1**), typically carried out as described in the following example.

The monomer, AIBN and THF were added into a dried reaction tube containing a magnetic stirrer bar. The molar ratio was set with $N_{monomer} : N_{AIBN} = 100 : 1$, and the monomer mass concentration was 25%. After three freeze-pump-thaw cycles, the tube was sealed under vacuum. Polymerization was carried out at 75 °C over 12h. The sample was purified by similarly re-precipitating three times from THF into methanol.

2.4. Instruments and measurements

Nuclear magnetic resonance (NMR). ^{1}H NMR measurements were performed on a Bruker ARX400 MHz

spectrometer using with $CDCl_3$ as solvent, tetramethylsilane (TMS) as the internal standard at room temperature.

Gel permeation chromatography (GPC). The apparent number average molecular weight (M_n) and polydispersity index (PDI = M_w/M_n) were measured on a GPC (WATERS 1515) instrument with a set of HT3, HT4 and HT5. The μ-styragel columns used THF as an eluent and the flow rate was 1.0 ml min^{-1} at 38 ^{o}C. The GPC data were calibrated with polystyrene standards.

Thermogravimetric analysis (TGA). TGA was performed on a TA SDT 2960 instrument at a heating rate of 20 ^{o}C min^{-1} in nitrogen atmosphere.

Differential scanning calorimetry (DSC). DSC traces of the polymers were obtained using a TA Q10 DSC instrument. The temperature and heat flow were calibrated using standard materials (indium and zinc) at a cooling and heating rates of 10 ^{o}C min^{-1}. The sample with a typical mass of about 5 mg was encapsulated in sealed aluminum pans.

Polarizing optical microscope (POM). LC texture of the polymer was examined under POM (Leica DM-LM-P) equipped with a Mettler Toledo hot stage (FP82HT).

One-dimensional wide-angle X-ray diffraction (1D WAXD). 1D WAXD experiments were performed on a BRUKER AXS D8 Advance diffractometer with a 40 kV FL tubes as the X-ray source (Cu Kα) and the LYNXEYE_XE detector. Background scattering was recorded and subtracted from the sample patterns. The heating and cooling rates in the 1D WAXD experiments were 10 ^{o}C min^{-1}.

Two-dimensional wide-angle X-ray diffraction (2D WAXD). 2D WAXD was carried out using a BRUKER AXS D8 discover diffractometer with a 40 kV FL tubes as the X-ray source (Cu Kα) and the VANTEC 500 detector. The point-focused X-ray beam was aligned either perpendicular or parallel to the mechanical shearing direction. For both the 1D and 2D WAXD experiments, the background scattering was recorded and subtracted from the sample patterns.
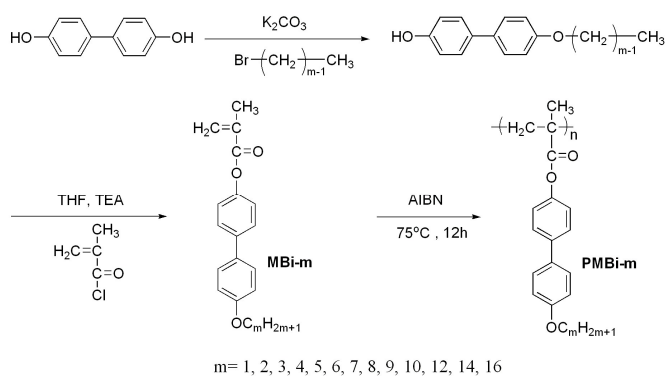
Scheme 1 Synthetic route of monomers (MBi-m) and corresponding polymers (PMBi-m).

3. Results and discussion

3.1. Synthesis and characterization of monomers and polymers

A series of methacrylate biphenyl monomers with the different lengths of alkyl tail (m= 1, 2, 3, 4, 5, 6, 7, 8, 9, 10, 12, 14, 16) were synthesized according to the synthetic route illustrated in **Scheme 1**. All polymers could be easily polymerized by free radical polymerization method. Herein, we use PMBi-10 as an example to elucidate the process. **Fig.3(a)** and **(b)** give the ^{1}H NMR spectra (CDCl$_3$) of the monomer MBi-10 and the polymer PMBi-10, respectively. The MBi-10 showed the characteristic resonances of the vinyl group at 5.71 and 6.42 ppm. In addition, the chemical shifts and peak integrations of all the protons in the monomer are in excellent agreement with its expected structure. Mass Spectrometry spectrums further confirmed the molecular structure. After polymerization, these signals disappeared completely. The chemical shifts of PMBi-10 were quite broad and consistent with the expected polymer structure. In order to the influence of M_n on the LC behavior, a series of polymers with the high M_n were synthesized. The M_n of these polymers ranged from 2.6×10^4 to 11.5×10^4 g/mol, with the polydispersity of 2.0-3.9 were measured by gel permeation chromatography (GPC) (**Table 1**). Meantime, all polymers showed good thermal stability, that was, the temperatures at 5% weight loss of the samples under nitrogen were about 310 ^{o}C measured by TGA at a rate of 20 ^{o}C/min. The molecular characterizations of the polymers are summarized **Table 1**.
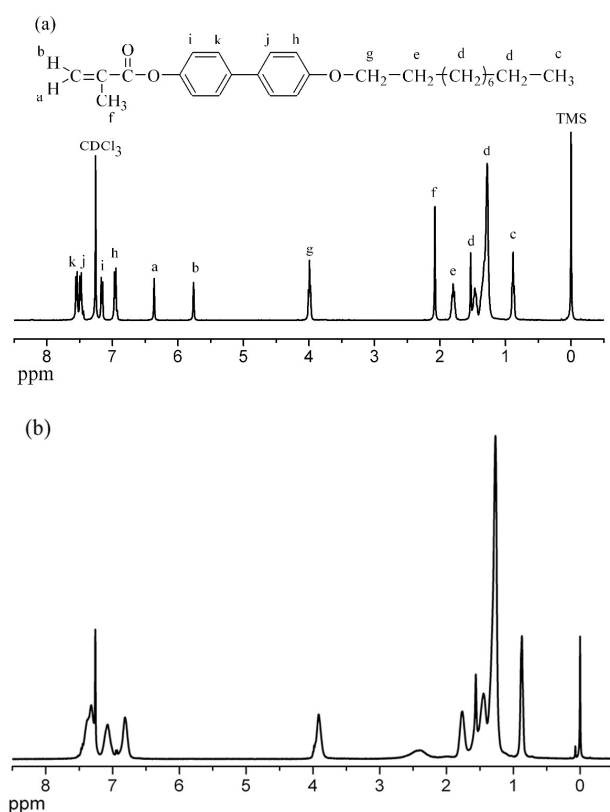
Fig.3 ^{1}H NMR spectrums of the monomer MBi-10 (a) and the polymer PMBi-10 (b) in CDCl$_3$.

3.2. Phase transitions and phase structures of the polymers

Fig.4 shows the second heating DSC curves of PMBi-m (m = 1, 2, 3, 4, 5, 6, 7, 8, 9, 10, 12, 14, 16) at a rate of 10 °C/min under nitrogen atmosphere after eliminating the thermal history. As can be seen from it, a weak second-order transition assigned as a glass transition for PMBi-m (m = 6, 7, 8, 9, 10, 12, 14, 16) and the glass transition temperature (T_g) decreased with the

Table 1 Molecular Characteristics of Polymers.

Sample	$M_n(\times10^4)^a$	PDI[a]	$T_g(^oC)^b$	$T_i(^oC)^c$	$T_2(^oC)^d$	$T_d(N_2)^e$
PMBi-1	6.5	2.1	--	295	304	320
PMBi-2	10.3	2.1	--	277	278	359
PMBi-3	8.5	2.4	--	288	286	342
PMBi-4	8.2	3.6	--	275	277	357
PMBi-5	6.2	2.0	--	266	259	350
PMBi-6	3.4	2.5	192	234	240	350
PMBi-7	10.4	2.3	202	259	265	325
PMBi-8	3.0	2.8	184	221	226	323
PMBi-9	11.5	2.4	175	245	250	315
PMBi-10	2.6	3.0	144	211	214	342
PMBi-12	5.8	3.9	121	217	209	341
PMBi-14	3.8	2.3	110	220	219	355
PMBi-16	6.0	3.9	96	221	226	362

a. Relative Mn and PDI were measured by GPC using PS standards.

b. The glass transition temperatures were measured by DSC at a heating rate of 10 °C/min under nitrogen atmosphere during the second heating process.

c. The transition temperature from liquid crystalline phase to isotropic phase measured by DSC at a heating rate of 10 °C/min under nitrogen atmosphere during the second heating process.

d. The transition temperature from liquid crystalline phase to isotropic phase measured by POM at a heating rate of 10 °C/min under nitrogen atmosphere during the second heating process.

e. The temperatures at 5% weight loss of the samples under nitrogen [$T_d(N_2)$] were measured by TGA heating experiments at a rate of 20 °C/min.

increasing of the alkyl tail length because of the plastification of the alkane (see **Fig.4(b)**). In high temperature, all polymers exhibited the board endothermic peak which was marked with the arrows (see **Fig.4(a)**). Combined the POM results, these transition peaks corresponded to the interconversion from the LC phase to isotropic phase (the clearing point, T_i) and the results are shown in **Table 1**. In low temperature, the PMBi-m (m=12, 14, 16) presented the crystalline melting peaks of the long alkyl tails. In addition, the PMBi-m (m=1, 2, 3, 4) showed the relatively broad peaks exists left before the clearing point. This phase structure transition process could be detected by POM except for the PMBi-1. For the PMBi-1, the POM and 1D WAXD showed that it only showed the smectic A (SA) phase. Therefore, this relatively broad peak may stand for a possible second order glass transition because this phenomenon can be found in other SCLCPs.[32]

POM experiments further study the LC phase structure of the PMBi-m. From the POM experiences, the polymers can be divided into three types. First one is PMBi-1. On cooling from the melt, this polymer showed a smectic schlieren texture (**Fig.5(a)**). Continue cooling, no new texture appeared, except that there was a little change of the colour of texture (**Fig.5(b)**).

The second one is PMBi-m (m=2, 3, 4). They exhibited two kinds of LC textures and POM results are shown in **Fig.5(c)** and **(d)**. After the samples were cooled from the isotropic state to below the isotropic temperature, a smectic schlieren texture was observed, which should correspond to the formation of SA phase at high temperatures (see **Fig.5(c)**). Continuing slowly cooling, the new LC texture appeared at 273 °C (see **Fig.5(d)**), suggesting the formation of a new LC phase. However, it is hard to estimate the LC phase structure. Second, the PMBi-m (m=6, 8, 10, 12, 14, 16) only formed the needle-like LC texture below the isotropic temperature and the results were shown in **Fig.5(e)**, **(f)**, **(g)** and **(h)**, indicating the formation of SA phase. The POM results were consistent with the DSC results.
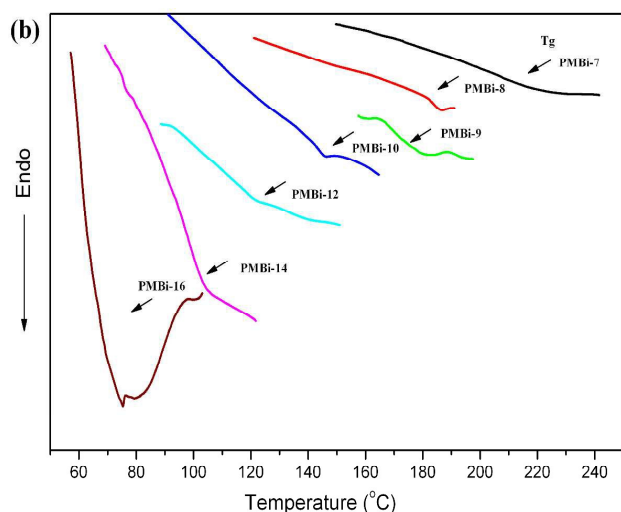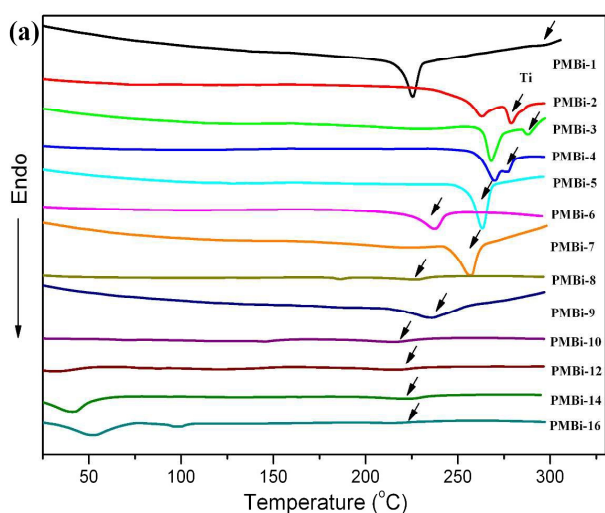
Fig.4 DSC curves of PMBi-m during the second heating scan at a rate of 10 ^{o}C min^{-1} under nitrogen atmosphere (a) and (b).
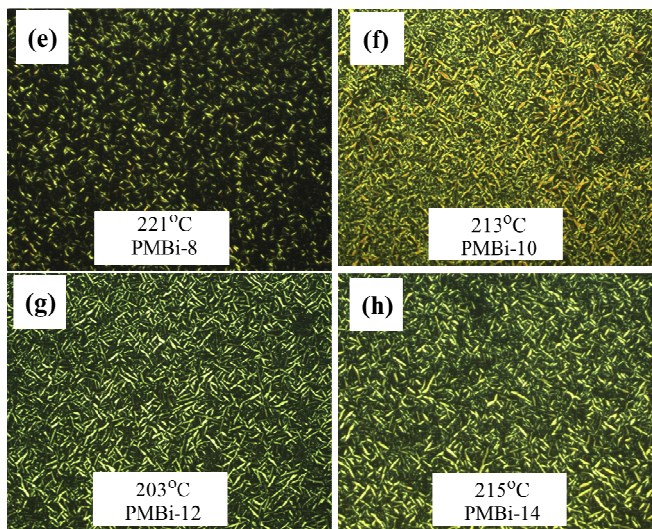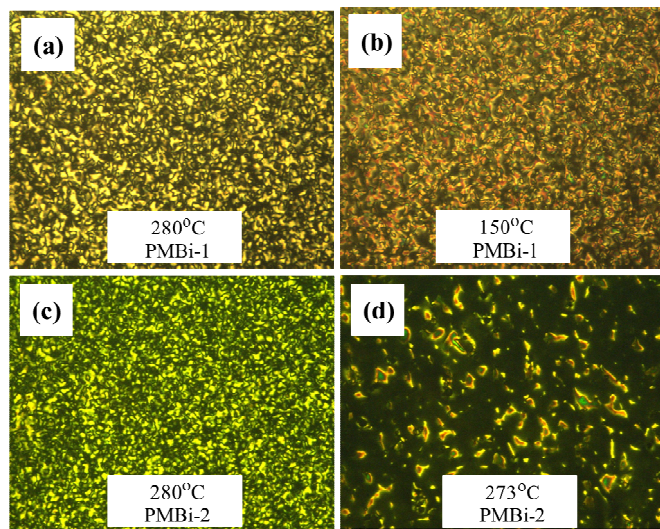
Fig.5 Representative POM images of the texture of the PMBi-1 maintained at 280 ^{o}C (a), 150 ^{o}C (b) and PMBi-2 maintained at 280 ^{o}C (c), 273 ^{o}C (d) and representative POM images of the texture of the PMBi-8~14 maintained at 221°C (e), 213 ^{o}C (f), 203 ^{o}C (g), 215°C (h). (Magnification: ×200)

1D WAXD analysis can provide useful information concerning molecular arrangement, mode of packing, and type of order in a mesophase of a polymeric LC. The 1D WAXD diffractogram of a powdery sample can be generally divided into the low-angle bragg reflections at 2θ=1.5-6° corresponding to the layer spacing of molecular orientational order and the high-angle peaks at 2θ=20° associated with the two-dimensional liquidlike intermesogenic organization within the layers. To be consistent with the DSC results, the samples were heated to the isotropic temperature, and then slowly cooled to the room temperature. 1D WAXD experiment results showed that the polymers could be divided into four types.

The first one is PMBi-1 and the 1D/2D WAXD were shown in **Fig.6**. **Fig.6(a)** presents a set of 1D WAXD patterns of PMBi-1 at different temperatures (from 30 ^{o}C to 250 ^{o}C) and we found that the missed first-order diffraction could be observed upon our 1D WAXD heating experiments. During the heating experiment, only two sharp diffractions at 10.8^{o} and 16.5^{o} are observed and the scattering vectors of the multiple peaks are found to follow a ratio of 2:3. Moreover, in the whole temperature, 1D WAXD patterns was the same, showing that the phase structure of polymer was not changed. In 2D WAXD results (**Fig.6(b)**), we further identified that the first-order diffraction was located on equator (2θ=5.3^{o}), confirming the LC phase of SA. Therefore, the PMBi-1 exhibited the stable SA phase below the clearing temperature. However, the absence of the first-order diffraction at low temperatures is ascribed to the possible matching of the electron densities between the center portion of the side-chain sublayer and the main-chain sublayer of the SA structure.[33]

(a)

(b)

fiber

X
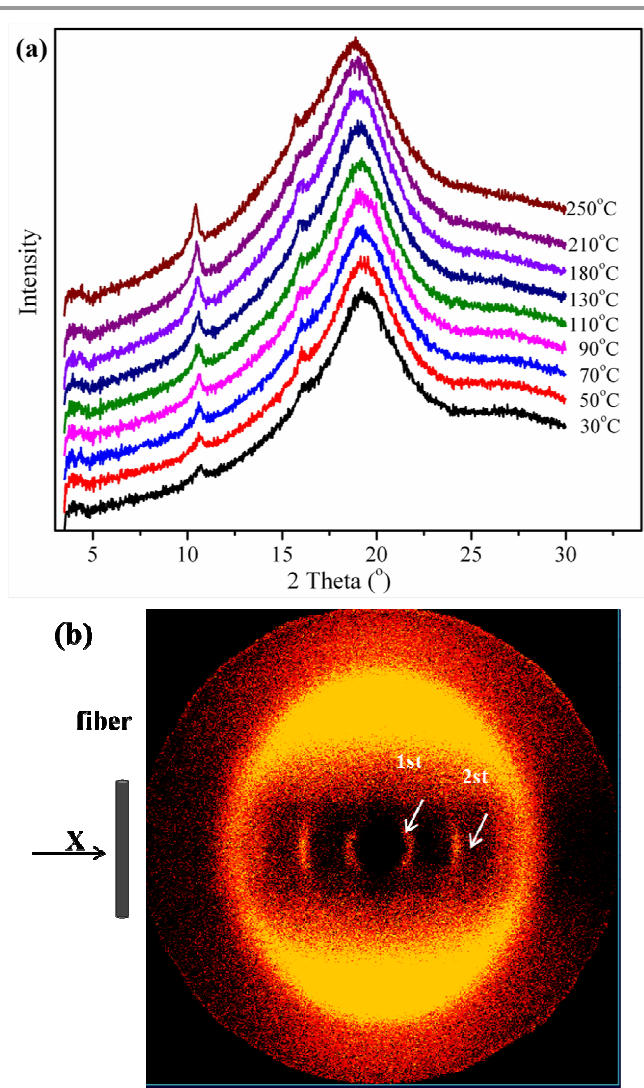
Fig.6 1D WAXD patterns of the PMBi-1 during the heating process of the as-cast film (a) and 2D WAXD patterns of the PMBi-1 at the fiber pattern at the room temperature (b).

The second one is PMBi-2, PMBi-3 and PMBi-4. **Fig.7(a)** describes the structurally sensitive 1D WAXD patterns of the PMBi-2 from 50 ^{o}C to 280 ^{o}C. As can be seen from it, in the low 2θ region, four obvious diffraction peaks are observed, with a ratio of scattering vector q (q = $4\pi \sin\theta/\lambda$, with λ the X-ray wavelength and 2θ the scattering angle) of 1:1.7:2.9:4.4. Interesting, the peak at 5.33^{o} is not as broad as those at 3.22^{o}, 9.34^{o}, and 14.17^{o}, meantime, the q-ratio of these four peaks is not equal to 1:2:3:4, indicating that the polymers exhibit two phase structures. To elucidate the packing of mesogens in the mesophase, the experimental interlayer distance was compared to the lamellar spacing L calculated using molecular modeling software from Material Studios 3.0. (L is the distance between a C-atom of the end-methyl group of the mesogen (full extended) and the carbon atom of the polymer chain.) The layer spacing derived from the Bragg reflection at 2θ=3.22^{o} (d_1=2.74nm) is longer than L (1.65 nm) of one monomer repeat unit of MBi-2, but smaller than 2L, suggesting a tilted bilayer lamellar structure (SmC). While the second peak at 2θ=5.53^{o} (d_2=1.61 nm) corresponds well to one

monomer repeat unit length (1.65 nm). Therefore, the LC phase structure of PMBi-2 maybe involves both mono- and bilayer packing arrangements, leading to partially responsible for two adjacent transition peaks for the DSC (see **Fig.4**) and for the difficulty in growing perfect LC textures (see **Fig.7(c)**). This phenomenon has been reported by Tang B. Z.[34] 2D WAXD further identify the phase structures. The 2D WAXD pattern of PMBi-2 recorded at 25 ^{o}C with the X-ray incident beam perpendicular to the fiber direction is shown in **Fig.7(b)**. In the high-angle region at 21.0^{o}, a pair of strong scattering halos is observed to be concentrated on equator, which is mainly resulted from the interference of side-chains which pack parallel to each other, indicating that the sample is well oriented. On the other hand, in the low-angle region, three low-angle spots, which should be correlated to the smectic layer diffraction, appears on meridian. As the chain backbones are aligned along equator, this

(a) heating

(b)

fiber

X
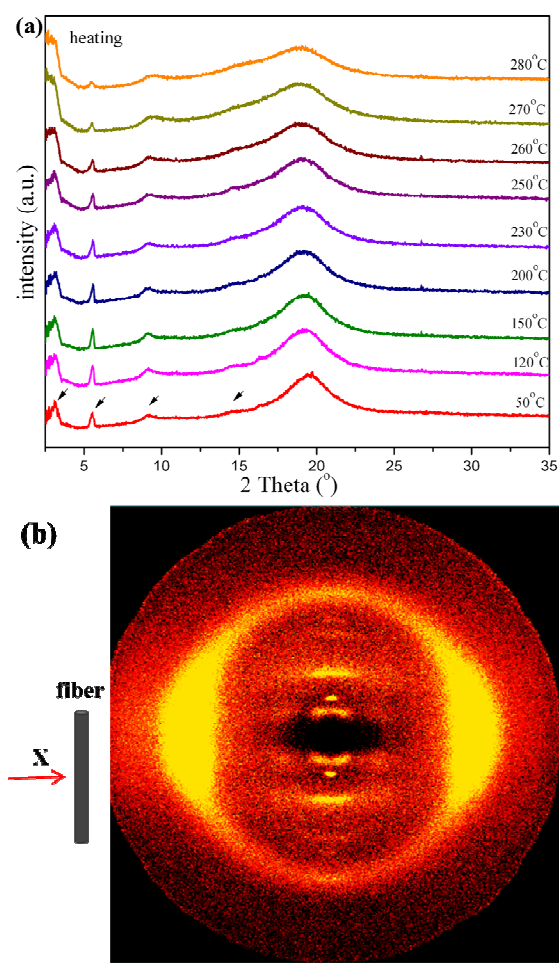
Fig.7 1D WAXD patterns of the PMBi-2 during the heating process of the as-cast film (a) and 2D WAXD patterns of the PMBi-2 at the fiber pattern at the room temperature (b).

diffraction pattern indicates that the mesogenic groups on side chains are parallel to the smectic layer normal. Surprised, in the low-angle region, four rather diffuse spots with 2θ of 3.2^{o} are located in quadrant, which imply some characteristics of an SmC structure.[5, 33] On the other hand, a pair of streaks can be observed at 9.4^{o}, which can be assigned as the third order diffraction for SmC phase.

The third one is PMBi-m (m=5, 6, 7, 8, 9, 10). **Fig.8(a)** and **(b)** illustrate the temperature-variable 1D WAXD patterns of PMBi-6 from 30 to 200 °C and from 200 to 30 °C in the 2θ region from 2.5° to 30°. At low angle, three narrow reflection peaks were observed. The scattering vectors of these peaks are found to follow a ratio of 1:2:3, indicating a smectic structure with a periodicity of 3.22 nm. Compared with the L of MBi-6 (2.15nm), the polymer formed bilayer smetic A phase, in which the alkyl tails are interdigitated in an antiparallel fashion.

The last one is PMBi-12, PMBi-14 and PMBi-16. With increasing the length of alkyl terminals, the crystallization phenomenon of longer alkyl tails could be detected by the 1D WAXD, so 1D WAXD experiments for PMBi-m (*m* = 12, 14 and 16) provided the different information about the changes of structural relative to the PMBi-m (*m* = 6, 8 and 10). Herein, we use the PMBi-16 as an example (see **Fig.9(a)** and **(b)**) to elucidate the structural evolution.

Fig.8 1D WAXD patterns of the PMBi-6 during the heating process (a) and the first cooling process (b) of the as-cast film.
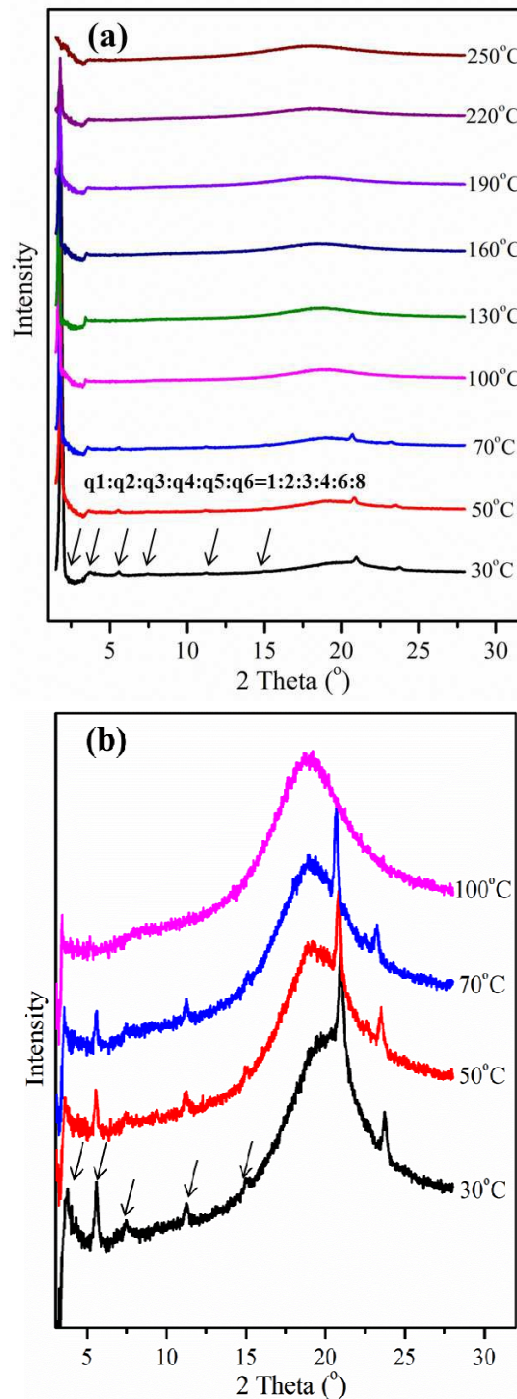
Fig.9 1D WAXD patterns of the PMBi-16 during the heating process of the as-cast film (a) and (b).

At lower temperature range the WAXD patterns only rendered several peaks (as shown in **Fig.9(b)**) in the high 2θ region of 17-30°, indicating the typical crystal formed by the long alkoxy tails. In the low 2θ region of 1.5-15°, seven obvious diffraction peaks were observed. The ratio of scattering vectors of these peaks was 1:2:3:4:6:8, indicating the polymer formed bilayer smectic A phase. When the sample was heated to 70 °C, several peaks in **Fig.9(b)** gradually disappeared, showing the alkyl tail entry into the isotropic phase. Thus, the enantiotropic phase transition sequence of PMBi-16 follows: the bilayer smetic A phase with the crystal of alkyl tail ↔ the bilayer smectic A phase ↔ isotropic phase. Based on the 1D WAXD, the d-spacing values of PMBi-m (m = 1, 2, 3, 4, 5, 6, 7, 8, 9, 10, 12, 14, 16) are shown in **Table 2**. As can be seen from it, the spacing of layers of the polymers increased with the increase of alkyl tail.

3.3. Phase transitions and phase structures of the polymers

Based on DSC, POM and 1D/2D WAXD experiments results, all polymers formed the smectic phase and the schematic drawing of phase structure of polymers is shown in **Fig.10.** For the PMBi-1, the Duran and Gramain et al have found that it presented the $S_{OB} \rightarrow S_A \rightarrow N \rightarrow I$ with the increase of temperature.[35-36] However, our polymer only showed the smectic A phase. As for this, it may be caused by the high M_n and the high viscosity of our polymers. **Fig.11** showed the dependence of the transition temperatures (T_g and T_i) on the length of alkyl tail, m, for the PMBi-m series (a) and on the length of spacer, m, for the poly[ω-(4'-methoxybiphenyl-4-yloxy)alkyl methacrylate]s (PMBiA-m) (b).[16, 37-38] Compared with the phase behavior of PMBiA-m, the PMBi-m presented the high T_g and T_i. As for this, it because that the formation of smetic phase structure was developed by the mesgoens and the main chain for the SCLCPs without spacer. For later, the polymers exhibited the smetic

phase owing to the decoupling and self-organization of the mesgoen moieties. On the other hand, the clearing temperatures decrease with a small odd-even effect as the length of the alkyl tail increases and then increase slightly. When the alkoxy tails were added to the mesgoen, the interaction of mesgoen can increase due to the dipole-dipole interaction, leading to the formation of LC phase. Meantime, the long flexible alkyl side chains were beneficial to the layered structures due to the unfavorable interaction between mesogens and the apolar alkyl side chains, leading to the stable of LC phase[39-40].
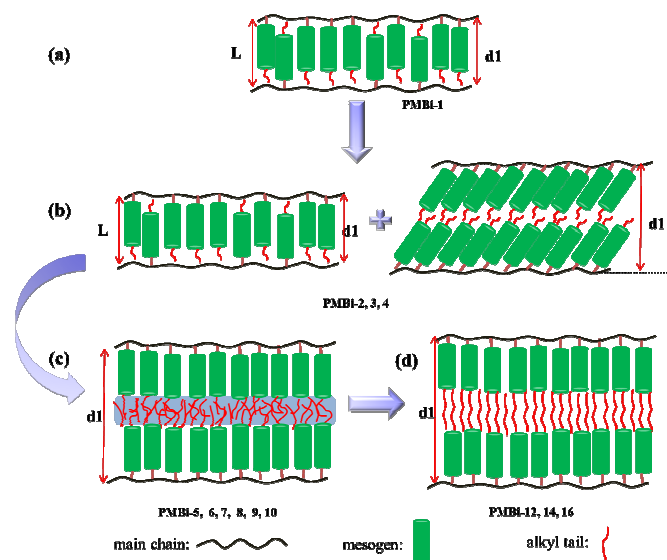
Fig.10 Possible liquid crystalline mesophase structures of PMBi-m.

Table 2 The 2θ, d-Spacing Values and Calculated Length of the Mesogenic Units.

Sample	$2\theta(°)^a$	d-spacing (nm)^a	Calculated Length of the Mesogenic Units (nm)^b
PMBi-1	5.30	1.67	1.51
PMBi-2	3.22	2.74	1.65
PMBi-3	3.24	2.72	1.76
PMBi-4	3.20	2.78	1.91
PMBi-5	2.88	3.07	2.01
PMBi-6	2.74	3.22	2.15
PMBi-7	2.51	3.52	2.26
PMBi-8	2.41	3.66	2.40
PMBi-9	2.30	3.84	2.51
PMBi-10	2.25	3.92	2.66
PMBi-12	2.15	4.11	2.91
PMBi-14	2.04	4.33	3.16
PMBi-16	1.93	4.58	3.41

^{a} Obtained from the 1D WAXD experiments.

^{b} Assuming the n-alkoxy tails in the side chains have an all-trans conformation.
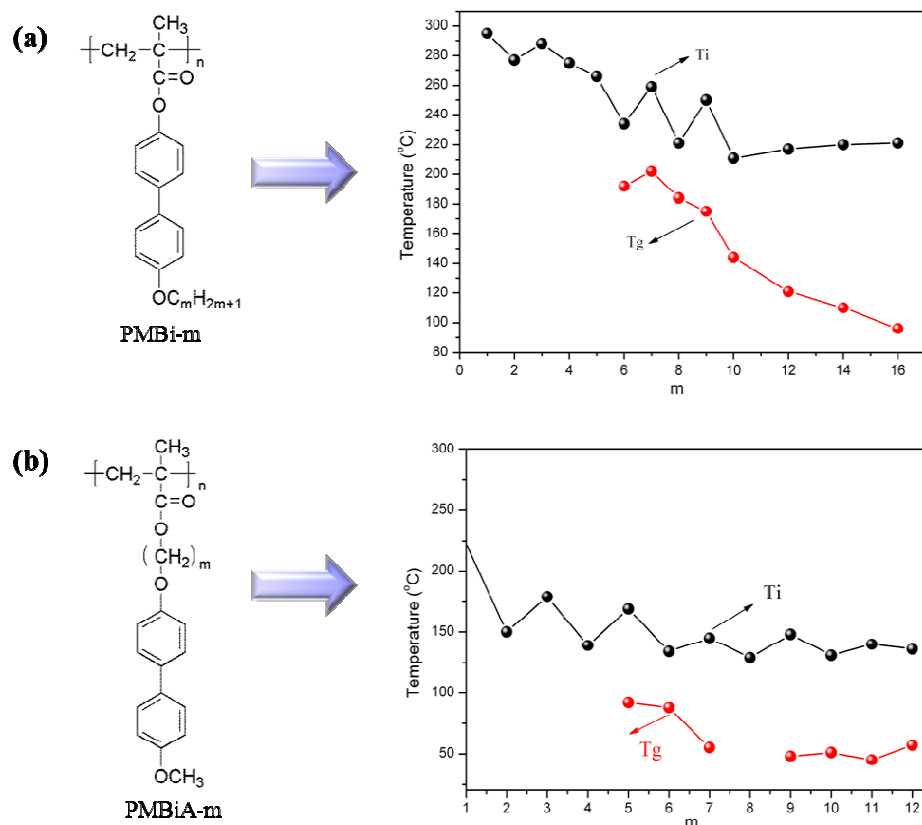
Fig.11 Dependence of the glass transition temperatures (T_g) and clearing temperatures (T_i) on the number m of methylene groups in the tail for PMBi-m (a) and in the spacer for PMBiA-m.

4. Conclusions

In summary, we have investigated the phase structures and transitions of a series of SCLCPs (PMBi-m, m =1, 2, 3, 4, 5, 6, 7, 8, 9, 10, 12, 14, 16) with the different alkyl tail lengths via DSC, POM and1D/2D WAXD. The results showed that the PMBi-m exhibited the stable smectic phase. Through studying, the alkyl tail plays an important role in the formation of LC phase structure for the SCLCPs without the spacer. Meantime, it is easier to synthesize the SCLCPs when the mesgoens are introduced into the polymer backbone in comparison with the synthesis of SCLCPs with the spacer, which is of great importance for real applications. At present, our group is having exploited its real applications, such as solid-solid phase transition polymer materials. And this work will be presented in the near future.

Acknowledgements

References

1   N. Gimeno, I. Pintre, M. Martínez-Abadía, J. L. Serrano and M. B. Ros, *RSC Adv.,* 2014, **4**, 19694.

2   P. Kohn, L. Ghazaryan, G. Gupta, M. Sommer, A. Wicklein, M. Thelakkat and T. Thurn-Albrecht, *Macromolecules*, 2012, **45**, 5676.

3   P. Deshmukh, M. Gopinadhan, Y. Choo, S. Ahn, P. W. Majewski, S. Y. Yoon, O. Bakajin, M. Elimelech, C. O. Osuji and R. M. Kasi, *ACS Macro. Lett.*, 2014, **3**, 462.

4   X. Q. Liu, J. Wang, S. Yang and E. Q. Chen, *ACS Macro. Lett.*, 2014, **3**, 834.

5   Z. Q. Yu, J. W. Y. Lam, C. Z. Zhu, E. Q. Chen and B. Z. Tang, *Macromolecules*, 2013, **46**, 588.

6   J. G. Rudick and V. Percec, *Accounts. Chem. Res.*, 2008, **41**, 1641.

7   A. G. Cook, R. T. Inkster, A. Martinez-Felipe, A. Ribes-Greus, I. W. Hamley and C. T. Imrie, *Eur. Polym. J*, 2012, **48**, 821.

8   A. Martinez-Felipe, Z. Lu, P. A. Henderson, S. J. Picken, B. Norder, C. T. Imrie and A. Ribes-Greus, *Polymer*, 2012, **53**, 2604.

9   B. M. Rosen, C. J. Wilson, D. A. Wilson, M. Peterca, M. R. Imam and V Percec, *Chem. Rev.*, 2009, **109**, 6275.

10 K. G. Gutiérrez-Cuevas, L. Larios-López, R. J. Rodríguez-González, B. Donnio and D. Navarro-Rodríguez, *Liq. Cryst.*, 2013, **40**, 534.

11 W. Wei, Y. Liu and H. Xiong. *Polymer*, 2013, **54**, 6793.

12 X. F. Chen, Z. H. Shen, X. H. Wan, X. H. Fan, E. Q. Chen, Y G Ma and Q F Zhou, *Chem. Soc. Rev.*, 2010, **39**, 3072.

13 J. F. Ban, S. Chen and H. L. Zhang, *RSC Adv.,* 2014, **4**, 54158.

14 J. F. Ban, S. Chen and H. L. Zhang, *Polym. Chem.,* 2014, **5**, 6558.

15 T. Ganicz and W. Stańczyk, *Materials*, 2009, **2**, 95.

16 A. A. Craig and C. T. Imrie, *Macromolecules*, 1995, **28**, 3617.

17 X. Li, L. Fang, L. Hou, L. Zhu, Y. Zhang, B. Zhang and H. Zhang, *Soft Matter*, 2012, **8**, 5532.

18 H. Finkelmann, H. Ringsdorf and J. H. Wendorff, *Makromol. Chem.*, 1978, **179**, 273.

19 H. Finkelmann and G. Rehage. *Adv. Polym. Sci.*, 1984, **60**, 97.

20 V. Frosini, G. Levita, D. Lupinacci and P L Magagnini, *Mol. Cryst. Liq. Cryst.*, 1981, **66**, 21.

21 E. C. Hsu, S. B. Clough and A. Blumstein. *Journal of Polymer Science: Polymer Letters Editio*, 1977, **15**, 545.

22 B. Wang, H. Du and J. Zhang, *Steroids*, 2011, **76**, 204.

23 V. Frosini and P. L. Magagnini, *Journal of Polymer Science: Polymer Physics Edition*, 1974, **12**, 23.

24 P. L. Magagnini, A. Marchetiti, F. Matera, G. Pizzirani and G. Turchi, *Eur. Polym. J.*, 1974, **10**, 585.

25 A. K. Alimoglu and A. Ledwith, *Polymer*, 1984, **25**, 1342.

26 Y. S. Lipatov, V. V. Tsukruk and V. V. Shilov, *Journal of Macromolecular Science, Part C: Polymer Reviews*, 1984, **24**, 173.

27 J. F. Zheng, Z. Q. Yu, X. Liu, X. F. Chen, S. Yang and E. Q. Chen, *J. Polym. Sci. Part A: Polym. Chem.*, 2012, **50**, 5023.

28 R. J. Rodríguez-González, L. Larios-López, D. Navarro-Rodríguez, C. Solano and G. Martínez-Ponce, *Mol. Cryst. Liq. Cryst.*, 2009, **511**, 1753.

29 V. P. Shibaev and N. Plat, *Adv. Polym. Sci.*, 1984, **60**, 173.

30 J. F. Zheng, X. Liu, X. F. Chen, X. K. Ren, S. Yang and E. Q. Chen, *ACS Macro. Lett.*, 2012, **1**, 641.

31 S. Chen, A. Ling and H. L. Zhang, *J. Polym. Sci. Part A: Polym. Chem.*, 2013, **51**, 2759.

32 M. Xie and C. Zhang, *Polymer Preprints*, 2007, **48**, 518.

33 X. Q. Zhu, J. H. Liu, Y. X. Liu and E. Q. Chen, *Polymer*, 2008, **49**, 3103.

34 W. Y. Jacky, L. X. Kong, Y. Dong, K. L. Kevin, C. Xu and B. Z. Tang, *Macromolecules*, 2000, **33**, 5027.

35 C. Chovino, D. Guillon and P. Gramain, *Polymer*, 1998, 39, 6385–6390.

36 R. Duran, D. Guillon, P. Gramain and A. Skoulios, *J. Phys. France*, 1988, **49**, 1455.

37 S. Koltzenburg, D. Wolff, J. Springer and O. Nuyken, *J. Polym. Sci. Part A: Polym. Chem.*, 1998, **36**, 2669.

38 A. A. Craig and C. T. Imrie, *J. Mater. Chem.*, 1994, **4**, 1705.

39 V. Percec and C. Pugh, In Side Chain Liquid Crystal Polymers; C. B. McArdle, Ed.; Chapman and Hall: New York, 1989; pp 30.

40 C. Pugh and A. L. Kiste, *Prog. Polym. Sci.,*1997, **22**, 601.